Bsp1p/Ypr171p is an adapter that directly links some synaptojanin family members to the cortical actin cytoskeleton in yeast

Sidonie Wicky, Sabine Frischmuth, Birgit Singer-Krüger*

Institute for Biochemistry, University of Stuttgart, Pfaffenwaldring 55, D-70569 Stuttgart, Germany

Received 29 November 2002; accepted 9 January 2003

First published online 30 January 2003

Edited by Ulrike Kutay

Abstract In this study we identified a novel protein, Bsp1p, that interacts directly with two yeast synaptojanins, Sjl2p and Sjl3p, but not with Sjl1p. The interaction takes place via the Sac1/polyphosphoinositide phosphatase domain, whose conserved C-terminal region is important for binding. Subcellular localization and genetic interactions revealed a function of Bsp1p in the cortical actin cytoskeleton. A fraction of Bsp1p was found to be membrane-associated. Studies with mutants of phosphatidylinositol 4-kinase, *PIK1*, suggested that the interaction with membranes is facilitated by phosphoinositides. We propose that Bsp1p is an adapter that links Sjl2p and Sjl3p to the cortical actin cytoskeleton.

Key words: Sjl protein; Polyphosphoinositide phosphatase; Phosphoinositides; Cortical actin; Signaling

1. Introduction

Inositol phosphates are among the most widespread second messenger molecules in eukaryotic cell signaling. Growing evidence suggests a key function for phosphoinositides in cell physiology [1,2]. The phosphorylation state of phosphoinositides is regulated by lipid kinases, their dephosphorylation by lipid phosphatases. Members of the synaptojanin family are highly conserved inositol polyphosphate 5′-phosphatases that are defined by three domains: an N-terminal domain, homologous to the yeast Sac1 protein, that for some synaptojanin members has been shown to exhibit polyphosphoinositide phosphatase (PPIP) activity [3,4], a central 5′-phosphatase domain, and a C-terminal proline-rich domain.

Mammalian synaptojanin 1 is highly enriched in brain, specifically at nerve terminals. The localization of synaptojanin 1 on synaptic vesicles [5] and its interaction with proteins implicated in synaptic vesicle endocytosis suggested that it plays a role in the endocytosis of synaptic vesicles. In neurons of synaptojanin 1-deficient mice, clathrin-coated vesicles accumulate suggesting that the 5′-phosphatase is required for the uncoating step [6]. In *Caenorhabditis elegans*, the unique synaptojanin ortholog is defined by the UNC-26 gene. Consistent with the results from mammals, unc-26 mutants exhibit defects in vesicle trafficking in all tissues, but most profoundly in synaptic termini [7]. Due to various defects in early steps of endocytosis [7], *C. elegans* synaptojanin appears to facilitate multiple steps of synaptic vesicle recycling.

The yeast *Saccharomyces cerevisiae* contains three synaptojanin family members, designated Sjl1p, Sjl2p, and Sjl3p (also known as Inp51p, Inp52p, Inp53p). Consistent with a role in endocytosis, the Δ*sjl2* Δ*sjl3* and, more profoundly, the Δ*sjl1* Δ*sjl2* mutant are defective in fluid phase uptake and receptor-mediated endocytosis [8]. Both mutants were characterized by other defects including an abnormal plasma membrane morphology, loss of actin organization and cell polarity [8–10].

Here we identify and characterize a novel protein, which physically binds to the Sac1 domain of Sjl2p and Sjl3p, but not to that of Sjl1p or Sac1p. Since this domain contains PPIP activity we named the protein Bsp1p (binding protein of synaptojanin PPIP domain). Localization studies and genetic data suggest a function of Bsp1p in the cortical actin cytoskeleton.

2. Materials and methods

2.1. Strains, media, and plasmids

Unless otherwise indicated, strains (Table 1) were grown in complete medium (YPD) or synthetic growth medium (SD medium) to early logarithmic phase at 30°C in a rotary shaker. DNA manipulations were by standard techniques. The plasmids used are listed in Table 2.

2.2. Two-hybrid screen

The reporter strain Y190 was sequentially transformed with pAS1-Sjl2–588 and the *S. cerevisiae* library DNAs [11]. For each reading frame, more than 2×10^6 transformants were screened for the expression of the *lacZ* gene after growth on SD-ura-trp-his/25 mM 3-amino-1,2,4-triazole (3AT) plates, covering the entire library at a >99% confidence level.

To test for the interaction between *BSP1* (pYPR171-C1#9) and the indicated *SJL* constructs, β-galactosidase activity (filter assay) and growth on SD-ura-trp-his/25 mM 3AT plates were analyzed. The expression of the Gal4-BD fusions was confirmed by immunoblotting using an anti-HA antibody.

2.3. Epitope tagging of ORFs

A *SJL1*- and *SJL2*-specific polymerase chain reaction (PCR) fragment, generated by amplification from plasmid pBS1539 with oligonucleotides described below, was inserted in the genome downstream of, and in frame with, the *SJL1* and *SJL2* ORF, respectively, by homologous recombination [12]. A similar PCR-based homologous recombination was used to insert the 3×HA and the 13×Myc epitope at the C-terminus of Bsp1p, respectively [13]. The selectable markers were the *Schizosaccharomyces pombe HIS5* and the *kan*^{r} gene, respectively. Transformants were purified and correct integration was verified by PCR.

*Corresponding author. Fax: (49)-711-685 4392.
E-mail address: singer-krueger@po.uni-stuttgart.de (B. Singer-Krüger).

0014-5793/03/$22.00 © 2003 Published by Elsevier Science B.V. on behalf of the Federation of European Biochemical Societies.
doi:10.1016/S0014-5793(03)00067-X

5′-TAP, SJL2 (5′-AACCCTGAACTAGAGAAGCTAAGCGTTCATCCATTGAAGCCTTGCGACCCCAATTCCATGGAAAAGAGAAG-3′); 3′-TAP, SJL2 (5′-GAACAACGGTATTTTCATAACAGCCATAGTAATACAGATCATGGTTTGAAAGGTCTACGACTCACTATAGGG-3′).

5′-TAP, SJL1 (5′-AGAGATCCCAATCCATTCGTTGAGAACGAAGATGAGCCACTTTTTATAGAAAGGTCCATGGAAAAGAGAAG-3′); 3′-TAP, SJL1 (5′-ACAATGATTTGGCAAAAAGTTCCAGCCAAAAATAGAGAGTACGCTCACAGCCGCTACGACTCACTATAGGG-3′).

5′-HA, YPR171 (5′-TTCACCCGAATAAAAATAGGACTCGTGGTCCCAGAAGAAAACTTCCAACACGCGTGGGAGCAGGGGCGGGTGC-3′); 3′-HA, YPR171 (5′-TGTTTCAGGGTTTGAATAGCCTGTAATTTTACTGCTATTTTCTAATAAGGGAGGAAGAGGTCGACGGTATCGATAAG-3′).

5′-MYC, YPR171 (5′-TTCACCCGAATAAAAATAGGACTCGTGGTCCCAGAAGAAAACTTCCAACACGCGTGCGGATCCCCGGGTTAATTAAC-3′); 3′-MYC, YPR171 (5′-TGTACGTACATACATGTGTAAAATACGGAGGTCTACTCTGTAGTTACATCGATGAATTCGAGCTCG-3′).

2.4. Co-immunoprecipitation experiments

Fifty OD_{600} units of BS906, BS1099 and BS1255 cells were lysed with glass beads [12]. After extraction with 0.1% NP40 (final concentration) for 20 min on ice, the lysates were spun at 14 000 rpm for 20 min. The supernatants were subjected to affinity purification via binding to IgG-Sepharose beads [12]. After extensive washing with IP buffer (6×1 ml), bound proteins were released by the addition of sodium dodecyl sulfate-polyacrylamide gel electrophoresis (SDS–PAGE) sample buffer at 95°C. The presence of TAP-Sjl1p, TAP-Sjl2p, and HA-Bsp1p in the immunoprecipitates was detected by immunoblotting using rabbit anti-mouse IgG and the monoclonal anti-HA antibody 16B12 (Babco) as primary antibodies.

2.5. Immunofluorescence microscopy

Indirect immunofluorescence microscopy was performed as described [14]. Mouse α-HA (1:1000), mouse α-GFP (Roche, 1:50), and rabbit α-Myc (Santa Cruz Biotechnology, 1:100) were used as primary antibodies, followed by Cy^{TM3}-conjugated anti-mouse Fab fragment (Jackson ImmunoResearch) and Alexa 488-conjugated anti-rabbit IgG (Molecular Probes).

2.6. Other methods

In vitro translated ^{35}S-labeled Bsp1p was transcribed and translated as described [15]. For glutathione *S*-transferase (GST) pulldown experiments, soluble GST fusion proteins were purified under native conditions according to the manufacturer's instructions. GST pulldown experiments were carried out as described [15]. Nycodenz gradient centrifugation of a 100 000×*g* pellet fraction was performed as described [15]. Visualization of filamentous actin with rhodamine phalloidin (Molecular Probes) was performed according to [16]. Pheromone internalization assays were carried out with biosynthetically labeled [^{35}S]α-factor using the 'pulse-chase' protocol [17].

3. Results

3.1. Identification of BSP1

We were interested in identifying proteins that are implicated in the function of yeast Sjl2p/Inp52p. Since no proteins were known that interact with the N-terminal Sac1 domain of synaptojanins, this region of Sjl2p was fused to the Gal4 DNA binding domain to generate a bait protein used to search for interacting proteins with the yeast two-hybrid system. In a screen of approximately 9×10^6 transformants more than 40 activating plasmids were isolated, of which at least 11 represented distinct clones. The sequence of all these clones matched the open reading frame (ORF) of *YPR171w*. Because of the interaction of the gene product with the PPIP domain of synaptojanin (see below), we named it Bsp1p. The protein has an apparent molecular weight of 65 kDa, a p*I* of 10.02 and contains no potential transmembrane domains. No obvious homologies with other proteins could be recognized using the heuristic BLAST algorithm or HMMER profile-based search methods.

3.2. Bsp1p interacts directly with Sjl2p in vitro and in vivo

To confirm the two-hybrid interaction biochemically, we measured the binding of in vitro translated ^{35}S-labeled Bsp1p to GST fusions that contained either the Sjl2p Sac1 domain (Sjl2–588), the Sjl1p Sac1 domain (Sjl1–524) or an unrelated protein, Ypt51p. As shown in Fig. 1A, ^{35}S-labeled Bsp1p was specifically recruited by GST-Sjl2–588 (lane 3, 100%), but not by the other two GST fusions (lane 1 [22%] and lane 2 [18%]).

Next, we asked whether the complex formation between Sjl2p and Bsp1p could be detected in vivo upon immunoprecipitation of epitope-tagged Sjl2p. To purify a potential complex, we inserted the tandem affinity purification (TAP) epitope tag including two IgG binding units of protein A at the 3′ end of the *SJL2* ORF. This version of Sjl2p was functional, because it could support normal growth in a strain lacking both *SJL1* and *SJL2*, which otherwise results in a strong growth defect [8–10]. TAP-tagged Sjl1p was generated simi-

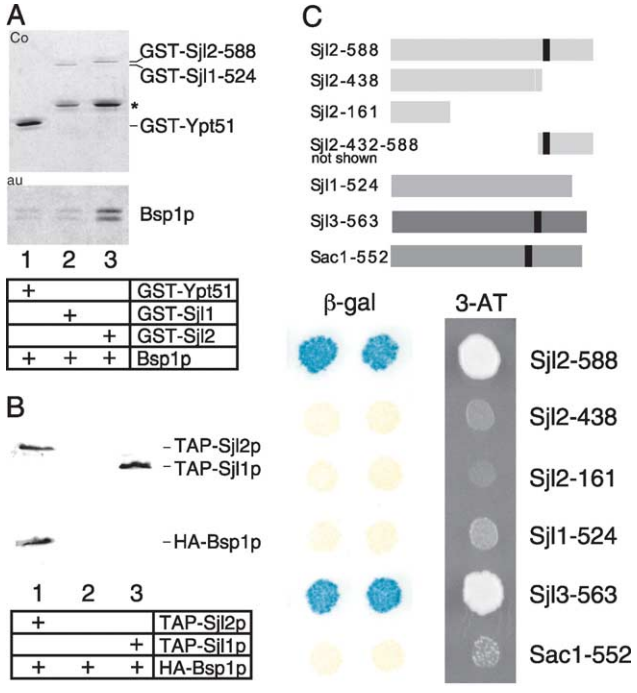

Fig. 1. Bsp1p interacts with the Sac1 domain of Sjl2p and Sjl3p, but not with that of Sjl1p and Sac1p. A: Purified GST fusions were immobilized onto glutathione *S*-transferase beads and incubated with in vitro translated [^{35}S]Bsp1p. After washing, bound proteins were eluted in SDS–PAGE sample buffer and separated by SDS–PAGE. Gels were stained with Coomassie brilliant blue (Co) to reveal the GST fusions, and processed for autoradiography (au) to visualize Bsp1p. The presence of two Bsp1p bands is due to a second methionine; asterisks indicate possible breakdown products. B: Co-immunoprecipitations were performed with cell extracts carrying the indicated epitope-tagged proteins. Proteins bound to IgG-Sepharose beads were released by boiling in SDS–PAGE sample buffer and detected by immunoblotting as described in Section 2. C: Two-hybrid interactions between combinations of pYPR171-C1#9 and pAS1-Sjl2–588, pAS1-Sjl2–438, pAS1-Sjl2–161, pAS1-Sjl1–524, pAS1-Sjl3–563, or pAS1-Sac1–552, respectively (as indicated in the schematic representation; the black bar represents the conserved $CX_5R(T/S)$ motif implicated in PPIP activity).

Table 1
Strains used

Yeast strain	Genotype	Source
BS64	*MAT***a** *his4 ura3 leu2 lys2 bar1-1*	[14]
RH1201	*MAT***a**/α *his4/his4 ura3/ura3 leu2/leu2 lys2/lys2 bar1-1/bar1-1*	H. Riezman, Basel, Switzerland
BS323	*MAT*α *his4 ura3 leu2 lys2 rvs167 bar1-1*	[16]
BS906	*MAT*α *ura3 leu2 lys2 BSP1::3×HA-HIS5* (*Schizosaccharomyces pombe*) *SJL2::TAP-URA3* (*Kluyveromyces lactis*)	this study
BS1099	*MAT***a** *ura3 leu2 lys2 BSP1::3×HA-HIS5* (*S. pombe*)	this study
BS1148	*MAT***a** *ura3 leu2 lys2 pik1-83::TRP1 BSP1::3×HA-HIS5* (*S. pombe*)	this study
BS1149	*MAT***a** *ura3 leu2 lys2 pik1-63::TRP1 BSP1::3×HA-HIS5* (*S. pombe*)	this study
BS1161	*MAT***a** *ura3 leu2 bsp1::kan^r abp1::kan^r*	this study
BS1173	*MAT***a** *his4 ura3 leu2 lys2 bsp1::kan^r rvs167 bar1-1*	this study
BS1255	*MAT***a** *ura3 leu2 lys2 BSP1::3×HA-HIS5* (*S. pombe*) *SJL1::TAP-URA3* (*K. lactis*)	this study
BS1261	*MAT***a** *ura3 leu2 lys2 BSP1::3×HA-HIS5* (S. pombe) *Δark1::HIS3 Δprk1::LEU2*	this study
BS1265	*MAT***a** *his4 ura3 leu2 lys2 BSP1::13×Myc-kan^r bar1-1*	this study
Y190	*MAT***a** *gal4 gal80 his3 trp1-901 ade2-101 ura3-52 leu2-3,-112+URA3::GAL→lacZ, LYS2::GAL→HIS3 cyh^r*	Steve Elledge, Houston, TX, USA

larly. To follow Bsp1p, a triple hemagglutinin (HA) epitope was inserted at its C-terminus.

TAP-Sjl1p and -Sjl2p assemblies were purified from total cellular lysates by affinity purification via IgG-Sepharose. The purified protein assemblies were separated by SDS–PAGE and analyzed by immunoblotting. HA-Bsp1p clearly copurified with TAP-Sjl2p (Fig. 1B, lane 1). The background of unspecifically bound HA-Bsp1p using an extract that contained non-tagged Sjl2p was very low (lane 2). As expected from the results in Fig. 1A, precipitation of TAP-Sjl1p did not lead to the co-purification of HA-Bsp1p (lane 3). Therefore, Bsp1p interacts with Sjl2p, but not Sjl1p, in vivo. The TAP-Sjl2p and HA-Bsp1p interaction was fully preserved when performing the original two-step tandem affinity purification [12] (data not shown), supporting the high efficiency and specificity of the interaction.

To define in more detail the region of the Sjl2-Sac1 domain that interacts with Bsp1p, a truncated version was generated in which the highly conserved $CX_5R(T/S)$ motif implicated in the PPIP activity of Sjl2p [3] was missing (Sjl2–438, Fig. 1C) and one in which only the N-terminal 161 amino acids remained (Sjl2–161). No two-hybrid interaction was observed between the truncated Sjl2p constructs and Bsp1p (Fig. 1C). Since the fusions were properly expressed, this suggested that the C-terminal end of the Sjl2p Sac1 domain may be relevant for the interaction with Bsp1p. However, it was not sufficient, since the 157 C-terminal amino acids of the Sjl2p Sac1 domain (amino acids 432–588) did not bind to Bsp1p (data not shown). Interestingly, Bsp1p also interacted with the PPIP-active Sjl3p Sac1 domain (Fig. 1C), but not with the PPIP-inactive Sjl1p Sac1 domain, either in the two-hybrid system (Fig. 1C), or in vitro or in vivo (Fig. 1A and B). Finally, the N-terminal domain of Sac1p did not interact with Bsp1p (Fig. 1C), although it was well expressed and contains PPIP activity [3]. Therefore, Bsp1p recognizes exclusively the Sac1 domains of two synaptojanin family members, Sjl2p and Sjl3p.

3.3. *Bsp1p localizes to cortical actin patches*

Localization of HA-Bsp1p by indirect immunofluorescence revealed a punctate staining pattern with cytoplasmic dots distributed over the entire cell. In small-budded cells the HA-Bsp1p-positive dots were brighter and more abundant within bud tips and at the cell periphery, suggesting a more concentrated localization at sites of active growth (Fig. 2A, arrowheads). HA-Bsp1p staining was also observed at the bud neck of large-budded cells (Fig. 2A, asterisks). Since the local-

Table 2
List of plasmids

Plasmid name	Characteristics	Source
pFA6a-13Myc-kanMX6	contains *13×Myc-kan^r*	[13]
p3×HA-HIS5	contains *3×HA-HIS5* (*S. pombe*) in pBSK-II	S. Munro, UK
pBS1539	contains *TAP-URA3* (*K. lactis*)	[12]
pDD667	contains *GFP-ACT1 URA3 CEN*	D. Drubin, USA
pAS1-Sjl2–588	*Bam*HI/*Sal*I fragment of *SJL2* (encodes amino acids 1–588) in pAS1	this study
pAS1-Sjl2–438	like pAS1-Sjl2–588, but encoding amino acids 1–438	this study
pAS1-Sjl2–161	like pAS1-Sjl2–588, but encoding amino acids 1–161	this study
pAS1-Sjl1–524	*Bam*HI/*Sal*I fragment of *SJL1* (encodes amino acids 1–524) in pAS1	this study
pAS1-Sjl3–563	*Bam*HI/*Sal*I fragment of *SJL3* (encodes amino acids 1–563) in pAS1	this study
pAS1-Sac1–552	*Bam*HI/*Sal*I fragment of *SAC1* (encodes amino acids 1–552) in pAS1	this study
pYPR171-C1#9	contains *YPR171w* in a modified pGAD424 [11]	this study
pYPR171#18	*BSP1*/*YPR171w* in pSEY8 (*URA3*, 2 μm), isolated from genomic pSEY8 library, includes *Eco*RI/*Nru*I fragment of *YPR171w*	this study
pGEX5-Ypt51	*Bam*HI/*Sal*I fragment of *YPT51* (encodes amino acids 1–210) in pGEX5-3	this study
pGEX5-Sjl2–588	*SJL2* subclone of pAS1-Sjl2–588 in pGEX5-3	this study
pGEX5-Sjl1–524	*SJL1* subclone of pAS1-Sjl1–524 in pGEX5-3	this study

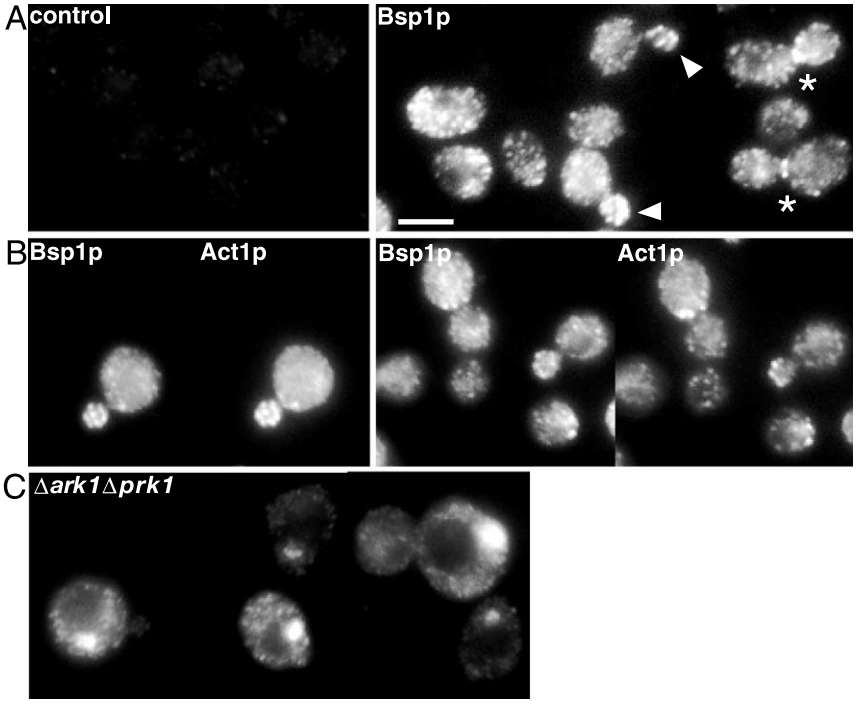

Fig. 2. Bsp1p is localized to actin cortical patches. A: Cells (BS64 and BS1099) were stained for HA-Bsp1p by indirect immunofluorescence as described in Section 2. Arrowheads and asterisks point to most intensive Bsp1p staining at the bud tips and necks, respectively; bar, 5 μm. B: Double indirect immunofluorescence using anti-Myc antibody to detect Myc-Bsp1p and anti-GFP antibody to detect GFP-Act1p. C: Localization of HA-Bsp1p in *Δark1 Δprk1* cells was performed as described in A.

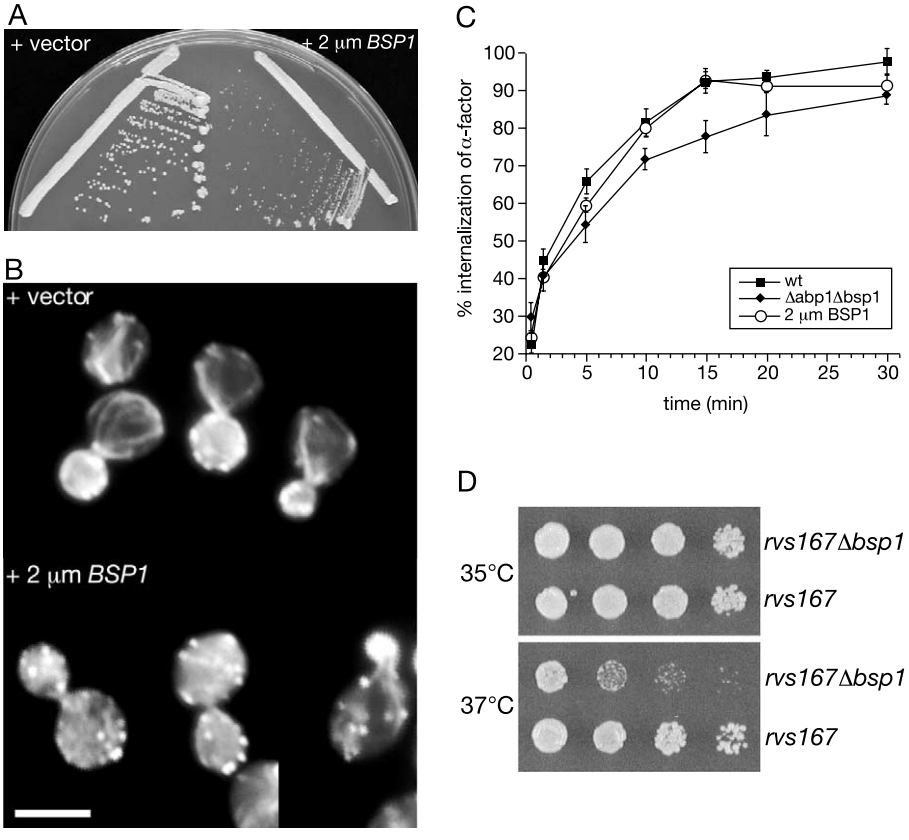

Fig. 3. Genetic interactions between *BSP1* and genes encoding actin cortical patch components. A,B: Overexpression of *BSP1* in wild-type cells results in a growth delay at 37°C (A) and in the mislocalization of actin cortical patches (B). In B, transformants, obtained after growth at 30°C, were fixed and stained with rhodamine-phalloidin; bar, 5 μm. C: [^{35}S]α-factor internalization assays were performed with the indicated strains as described in Section 2. D: A dilution series of *rvs167* and *rvs167 Δbsp1* cells after growth at 35°C and 37°C on YPD plates is shown.

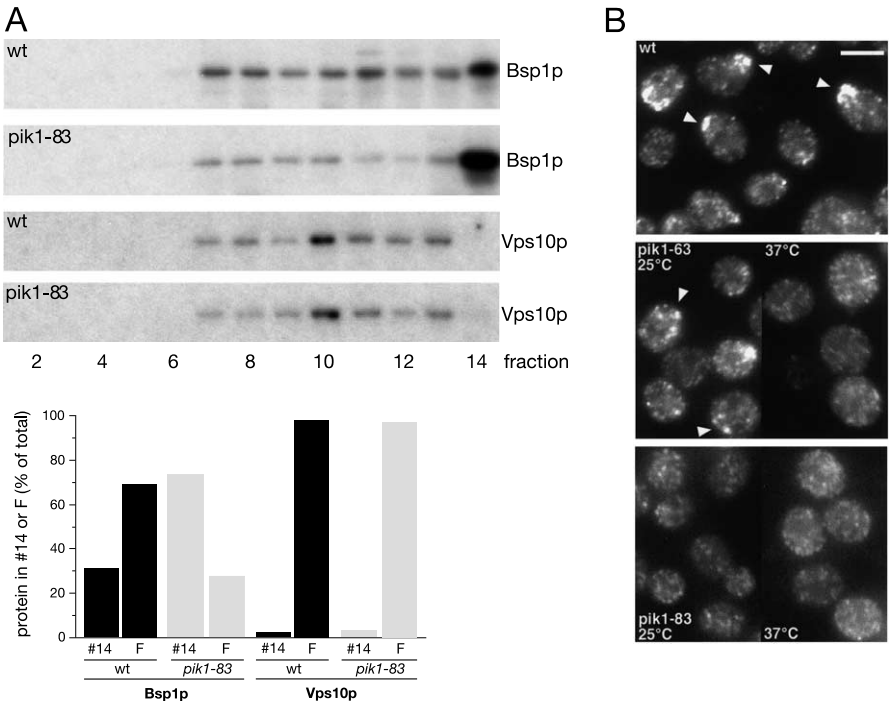

Fig. 4. The association of HA-Bsp1p with membranes and cortical patches is dependent on phosphoinositides. A: The 100 000×*g* pellet fractions generated from different cell lysates (BS1099 and BS1148) were each subjected to flotation into a Nycodenz gradient as described in Section 2. The presence of HA-Bsp1p and Vps10p in each fraction was determined by immunoblotting using [^{125}I]protein A. The immunoreactive bands were quantified with the phosphorimager (Molecular Dynamics). #14, fraction 14 (non-floated); F, fractions 1–13 (floated). B: After growth at the permissive temperature, cells were processed either directly for indirect immunofluorescence or shifted to 37°C for 2 h prior to the fixation and staining as described in Fig. 2. Arrowheads point to regions of intense Bsp1p staining; bar, 5 μm.

ization pattern was similar to that of the cortical actin cytoskeleton, to which synaptojanins are functionally connected [8,18], we determined whether the HA-Bsp1p-positive structures contained actin. Cells expressing HA-Bsp1p and GFP-Act1p were stained by double indirect immunofluorescence. There was a striking similarity between the staining patterns of HA-Bsp1p and GFP-Act1p (Fig. 2B). In particular, the dotted structures concentrated in bud tips and at the presumptive bud sites were mostly positive for both Bsp1p and Act1p.

Further independent evidence for a localization of Bsp1p to actin cortical patches came from analyzing the HA-Bsp1p staining pattern in the kinase-deficient Δ*ark1* Δ*prk1* mutant, in which the formation of cortical patch structures is drastically impaired [19]. In this mutant the HA-Bsp1p staining pattern collapsed into large aggregates (Fig. 2C) similar to the cytoplasmic actin clumps, to which other cortical patch components were found to mislocalize as well [19].

3.4. *Bsp1p is functionally connected to actin cortical patches*

In contrast to *BSP1*-deleted cells that exhibited no growth defects under a variety of conditions (data not shown), the overexpression of *BSP1* from a multicopy 2 μm plasmid led to a number of physiological alterations. Upon growth at 37°C *BSP1*-overexpressing cells were slightly temperature-sensitive (Fig. 3A) and in liquid culture at 30°C the generation time of *BSP1*-overexpressing cells increased to 3.6 h as compared to 2.1 h for cells containing the vector alone (data not shown). Because Bsp1p localizes to actin cortical patches (Fig. 2), we investigated the physiological consequence of *BSP1* overexpression on actin organization. In wild-type, the majority of cells with small and medium size buds (98%, $n=153$) displayed actin cables in the mother cell aligned toward cortical actin patches concentrated in the bud, similar to previously published staining patterns (Fig. 3B). In contrast, in cells overexpressing *BSP1* the highly polarized arrangement of cortical patches was impaired. Approximately 45% ($n=158$) of *BSP1*-overexpressing cells with small and medium size buds exhibited a mislocalization of cortical actin patches into the mother cells (Fig. 3B).

Because mutants in actin patch components are frequently defective in endocytosis [20], the endocytic internalization of the pheromone α-factor was analyzed. Δ*bsp1* (not shown) and *BSP1*-overexpressing cells (Fig. 3C) revealed no change in the kinetics of α-factor internalization. This suggested that either Bsp1p is not required for this transport reaction or its function in endocytosis is redundant. This is for example the case for the cortical patch component Abp1p [21], whose deletion causes no endocytic defect [22]. To test for a redundant function of Abp1p and Bsp1p in endocytosis, the kinetics of α-factor internalization were analyzed in the Δ*abp1* Δ*bsp1* strain. The rate of endocytosis was slightly but reproducibly reduced as compared to wild-type (Fig. 3C). Therefore, Bsp1p and Abp1p appear to have related functions in early steps of endocytosis. The combined deletion of *BSP1* and *ABP1* is, however, not yet sufficient to cause strong phenotypes.

Rvs167p, homologous to mammalian amphiphysin, is another cortical patch component that displays multiple two-hybrid interactions with proteins of related function [23]. While at 35°C, Δ*bsp1 rvs167* cells grew indistinguishably

from *rvs167* cells, at 37°C the double mutant exhibited an enhanced temperature sensitivity when compared to the *rvs167* strain (Fig. 3D). Consistent with the localization of Bsp1p to the cortical actin cytoskeleton, the harmful effect of *BSP1* overexpression on polarized actin patch localization and the genetic interactions between *BSP1* and genes encoding cortical patch components further corroborate a function of Bsp1p in the cortical actin cytoskeleton.

3.5. Effect of reduced levels of phosphatidylinositol (PtdIns) (4)P and PtdIns(4,5)P_2 on the subcellular localization of Bsp1p

Although Bsp1p is predicted to contain no transmembrane domains, upon subcellular fractionation it did not fractionate like a soluble, cytosolic protein but was found to sediment (data not shown). To further prove an association with membranes, the 100 000 × *g* pellet (P3), in which Bsp1p was found, was subjected to flotation into a Nycodenz density gradient. This showed that approximately 70% of the P3-associated HA-Bsp1p floated with membranes that contained the late Golgi marker Vps10p (Fig. 4A), Kex2p and the early endosome marker Ypt51p (data not shown). Due to the physical interaction between Bsp1p and synaptojanin proteins, we analyzed whether the membrane association of Bsp1p was dependent on phosphoinositides. *PIK1* encodes a PtdIns(4)P kinase which is implicated in membrane trafficking from the Golgi complex, but not in the organization of actin [24–26]. Interestingly, in cells carrying a mutant allele of *PIK1*, *pik1-83*, in which the levels of PtdIns(4)P and PtdIns(4,5)P_2 drop by 45–60% [24,26], the fraction of HA-Bsp1p that floated was significantly reduced (Fig. 4A). In contrast, the flotation of an integral membrane protein, Vps10p, was unaltered in the mutant.

To confirm this result with an alternative method, the localization of HA-Bsp1p was analyzed in two *pik1* mutants by indirect immunofluorescence after growth at 25°C, or after a 2 h shift at 37°C. While in wild-type the HA-Bsp1p staining pattern was not affected at 37°C (Fig. 4B), *pik1-63* cells incubated at the non-permissive temperature exhibited a clear reduction in the staining intensity of the larger Bsp1p-positive dots concentrated within bud tips (Fig. 4B, 37°C). At 25°C, the staining pattern was not yet affected. However, in agreement with reduced PtdIns(4)kinase activity in *pik1-83* already at 25°C [26], a diminished Bsp1p staining was already seen at the permissive growth temperature and at 37°C (Fig. 4B). Therefore, the association of Bsp1p with membranes and cortical patches correlated with the levels of PtdIns(4)P and PtdIns(4,5)P_2.

4. Discussion

In this study we identified a novel protein, Bsp1p, which directly interacts with the Sac1 domain of Sjl2p as detected by three independent assays: the two-hybrid system, an in vitro binding assay and co-immunoprecipitation. This is strong evidence for a physiologically relevant interaction between the two proteins. Interestingly, Bsp1p was also found to interact with the Sac1 domain of Sjl3p, but not with that of Sjl1p or Sac1p. It is possible that the Bsp1p–Sjl2p/Sjl3p interaction is somehow connected to the intrinsic PPIP activity of these two family members, because removal of the critical C-terminal region of the Sjl2 Sac1 domain implicated in this activity [3] abolished the interaction with Bsp1p. In this case, another synaptojanin-specific feature of the Sjl2p and Sjl3p Sac1 domains may be additionally required, because the PPIP-active Sac1 domain of Sac1p did not interact. This would also be consistent with the finding that the C-terminal end of the Sjl2 Sac1 domain with the PPIP consensus was not sufficient to allow binding to Bsp1p. It is also conceivable that Bsp1p recognizes a similar three-dimensional structure inherent to Sjl2p and Sjl3p independent of their PPIP activity. Further studies will be required to understand the functional basis for these specific interactions.

Our results and data from other laboratories strongly indicate that Bsp1p functions in the cortical actin cytoskeleton. The evidence ranges from localization to cortical patches and colocalization with actin (Fig. 2) and Abp1p [22] to the impairment of polarized actin organization in cells overexpressing *BSP1* (Fig. 3B). Furthermore, we provide evidence for genetic interactions between *BSP1* and *ABP1*, *RVS167*, and *ARK1PRK1*, respectively, while in a previous screen Bsp1p showed a two-hybrid interaction with the cortical patch components Cap1p, Rvs167p, and Sla1p [22]. Bsp1p seems to fulfill a function that is redundant with several other cortical patch components, since growth and endocytosis were only partially impaired in the double mutants that were studied. This supports the notion of a very large and complex network of interacting components within actin cortical patches. The challenge will be to elucidate the separate functions of individual components within this system.

The evidence for a direct physical interaction between synaptojanin proteins and a cortical patch component is novel. Although circumstantial evidence implicated synaptojanin proteins in the organization of the actin cytoskeleton, to our knowledge a physical interaction between a synaptojanin family member and a protein implicated in actin dynamics has been identified only in the case of mammalian synaptojanin 2 and the small GTPase Rac1 [27]. In yeast, rapid translocation of yeast Sjl2p and Sjl3p to actin cortical patches was previously described under conditions of hyperosmotic stress, but was found to occur independently of the polymerization state of actin by an unknown mechanism [18]. Thus, Bsp1p represents the first actin cortical patch component for which a direct physical link to Sjl2p (and probably Sjl3p) has been revealed under physiological conditions.

The finding that Bsp1p also interacts with membranes is interesting. Our results with the PtdIns(4)P kinase-deficient *pik1* mutants hint at a role of phosphoinositides in mediating the interaction with Bsp1p. Since the actin cytoskeleton is not affected in *pik1* mutants [26], the decreased Bsp1p patch-like staining was probably not caused by the mislocalization or dissociation of cortical patch components. Rather, we assume that the reduced PtdIns(4)P and PtdIns(4,5)P_2 levels affected the membrane association of Bsp1p either directly or via another linker. It is unlikely that Bsp1p interacts with membranes solely via synaptojanins, because of their lipid phosphatase activity. Rather, phospholipids and membrane-associated Sjl2p (and potentially also Sjl3p) may provide independent attachment sites for Bsp1p. Thus, Bsp1p could act as an adapter between the cortical actin cytoskeleton and sites of endocytic membrane traffic.

Acknowledgements: We are most grateful to Drs. Philip James, Jeremy Thorner, Sean Munro, Bertrand Séraphin, and David Drubin

for providing reagents used in this study. We acknowledge Hans Rudolph for critical reading of the manuscript and Dieter H. Wolf for helpful suggestions. This work was supported by a grant from the DFG to B.S.-K. (SFB495).

References

[1] Simonsen, A., Wurmser, A.E., Emr, S.D. and Stenmark, H. (2001) Curr. Biol. 13, 485–492.
[2] Cremona, O. and De Camilli, P. (2001) J. Cell Sci. 114, 1041–1052.
[3] Guo, S., Stolz, L.E., Lemrow, S.M. and York, J.D. (1999) J. Biol. Chem. 274, 12990–12995.
[4] Hughes, W.E., Woscholski, R., Cooke, F.T., Patrick, R.S., Dove, S.K., McDonald, N.Q. and Parker, P.J. (2000) J. Biol. Chem. 275, 801–808.
[5] Haffner, C., Takei, K., Chen, H., Ringstad, N., Hudson, A., Butler, M.H., Salcini, A.E., Di Fiore, P.P. and De Camilli, P. (1997) FEBS Lett. 419, 175–180.
[6] Cremona, O., Di Paolo, G., Wenk, M.R., Luthi, A., Kim, W.T., Takei, K., Daniell, L., Nemoto, Y., Shears, S.B. and Flavell, R.A. et al. (1999) Cell 99, 179–188.
[7] Harris, T.W., Hartwieg, E., Horvitz, H.R. and Jorgensen, E.M. (2000) J. Cell Biol. 150, 589–600.
[8] Singer-Krüger, B., Nemoto, Y., Daniell, L., Ferro-Novick, S. and De Camilli, P. (1998) J. Cell Sci. 111, 3347–3356.
[9] Srinivasan, S., Seaman, M.N., Nemoto, Y., Daniell, L., Suchy, S.F., Emr, S.D., De Camilli, P. and Nussbaum, R. (1997) Eur. J. Cell Biol. 74, 350–360.
[10] Stolz, L.E., Huynh, C.V., Thorner, J. and York, J.D. (1998) Genetics 148, 1715–1729.
[11] James, P., Halladay, J. and Craig, E.A. (1996) Genetics 144, 1425–1436.
[12] Rigaut, G., Shevchenko, A., Rutz, B., Wilm, M., Mann, M. and Seraphin, B. (1999) Nat. Biotechnol. 17, 1030–1032.
[13] Longtine, M.S., McKenzie, A., Demarini, D.J., Shah, N.G., Wach, A., Brachat, A., Philippsen, P. and Pringle, J.R. (1998) Yeast 14, 953–961.
[14] Singer-Krüger, B., Stenmark, H. and Zerial, M. (1995) J. Cell Sci. 108, 3509–3521.
[15] Jochum, A., Jackson, D., Schwarz, H., Pipkorn, R. and Singer-Krüger, B. (2002) Mol. Cell. Biol. 22, 4914–4928.
[16] Singer-Krüger, B. and Ferro-Novick, S. (1997) Eur. J. Cell Biol. 74, 365–375.
[17] Dulic, V., Egerton, M., Elguindi, I., Raths, S., Singer, B. and Riezman, H. (1991) Methods Enzymol. 194, 679–710.
[18] Ooms, L.M., McColl, B.K., Wiradjaja, F., Wijayaratnam, A.P., Gleeson, P., Gething, M.J., Sambrook, J. and Mitchell, C.A. (2000) Mol. Cell. Biol. 20, 9376–9390.
[19] Cope, M.J., Yang, S., Shang, C. and Drubin, D.G. (1999) J. Cell Biol. 144, 1203–1218.
[20] Wendland, B., Emr, S.D. and Riezman, H. (1998) Curr. Biol. 10, 513–522.
[21] Wesp, A., Hicke, L., Palecek, J., Lombardi, R., Aust, T., Munn, A.L. and Riezman, H. (1997) Mol. Biol. Cell 8, 2291–2306.
[22] Kübler, E. and Riezman, H. (1993) EMBO J. 12, 2855–2862.
[23] Drees, B.L., Sundin, B., Brazeau, E., Caviston, J.P., Chen, G.C., Guo, W., Kozminski, K.G., Lau, M.W., Moskow, J.J. and Tong, A. et al. (2001) J. Cell Biol. 154, 549–571.
[24] Hama, H., Schnieders, E.A., Thorner, J., Takemoto, J.Y. and DeWald, D.B. (1999) J. Biol. Chem. 274, 34294–34300.
[25] Walch-Solimena, C. and Novick, P. (1999) Nat. Cell Biol. 1, 523–525.
[26] Audhya, A., Foti, M. and Emr, S.D. (2000) Mol. Biol. Cell 11, 2673–2689.
[27] Malecz, N., McCabe, P.C., Spaargaren, C., Qiu, R., Chuang, Y. and Symons, M. (2000) Curr. Biol. 10, 1383–1386.